Milling robot modal analysis using spindle-driven unbalanced excitation in context of its response nonlinearity

G. Altshul [1], **M. Guskov** [1], **E. Balmes** [1,2], **P. Lorong** [1]
[1] PIMM, Arts et Metiers, CNRS, Cnam, HESAM,
151 Bd. de l'Hopital, 75013 Paris, France

[2] SDTools, 44 rue Vergniaud, 75013 Paris, France
e-mail: **grigorii.altshul@ensam.eu**

Abstract
This article presents a novel modal analysis method for investigating the dynamic behavior of milling robots. The proposed method utilizes inertial forces generated by an unbalanced tool rotating on the spindle to excite vibrations, and the frequency response function (FRF) is obtained through demodulation of the recorded vibrations. The study demonstrates the evolution of the robot's FRF with varying levels of unbalance, showing that the modes exhibit softening behavior and increased damping as the unbalance increases. The method offers a balance between simplicity and precision, requiring less instrumentation than operational modal analysis (OMA) methods while allowing for controlled excitation levels. The importance of precise spindle rotation speed data is highlighted, suggesting the benefits of using spindles with encoders for better results. This method can be applied for characterization of robots in different poses, addressing non-linear behavior significant for the robot's role in milling processes.

1 Introduction

Robots used as a support for machining allow for easier integration of milling operations into the manufacturing line, offering a broader working area and a wider choice of tool orientations compared to classical CNC machines. Hence, potentially, robotic milling reduces the cost of production for various industries. However, the widespread integration of robotic machining in industrial processes is constrained by their relatively high structural flexibility, both static and dynamic, inherent in their serial structure. This drawback leads to deterioration of the machined surface due to forced vibrations and makes nefarious phenomena, such as machining chatter, more probable.

In this context, the identification of the robot's dynamic behavior is a crucial step necessary for machining process modeling. One of the first approaches used for this was the characterization of robot static stiffness. Dumas et al. in [1] and [2] propose applying static forces and torques to the robot end-effector and then defining a criterion that allows selecting optimal robot poses from the perspective of static deformations. Olabi in [3] opts for another approach that consists of a series of static loadings on each robot axis while fixing the other axes. However, such approaches, though useful for approximating the stiffness of robot elements, without considering the robot's inertia, allow only for the compensation of only static deformation, completely ignoring possible phenomena arising from the system's dynamic behavior.

The dynamical properties of robots can be obtained through Experimental Modal Analysis (EMA), which allows the extraction of the robot's modal frequencies, damping ratios, and deformed shapes, considering the dynamic behavior of the robot as linear. The most widespread EMA method is hammer impact testing, which can be applied to extract the robot's frequency response function (FRF) in the modal domain and the corresponding modal parameters ([4, 5, 6]). These parameters can then be used for simulating robotic milling processes and stability analysis. In the work [7], the authors go further by using the robot's inertial data to

identify the robot axes stiffness using its FRF. They then use this data to approximate the robot's tool-tip FRF for different robot poses.

However, it has been shown that cutting conditions and tool rotations influence the dynamics of the robot and its FRF. Consequently, researchers have shown interest in operational modal analysis (OMA), which leverages cutting forces appearing during special milling experiments to sufficiently excite vibrations of the robot. Since the typical teeth passage frequency is much higher than the robot's modal frequencies, researchers tend to eliminate the spectrum content related to the harmonics of teeth engagement frequencies. Therefore, not all machining operations are suitable for FRF extraction and one of the approaches involve designing a milling process where cutting forces approximate random excitation.

Cai et al. [8] performed face milling of a narrow, randomly-curved band to create random excitation and discussed the elimination of excitation harmonics (teeth engagement that leaks into the recorded signal). Altun et al. [9] introduced a comprehensive method for Frequency Response Function (FRF) identification using cutting forces as excitation. Instead of measuring the milling forces directly, they are calculated using a mechanistic cutting force model. The methodology is divided into two parts: (i) identifying force coefficients with an a priori known point FRF, and (ii) identifying FRFs at other positions using the calculated milling force. The authors employed face milling with low radial engagement as the cutting geometry, considering the cutting force from each tooth engagement as a separate impact. Iglesias et al. [10] proposed using a series of different milling operations with spindle rotation speed sweep. In particular, for the case of the planar robot, they used up-milling, down-milling, and slot milling along with a rotary dynamometric tool holder to extract the robot's FRF in a specific configuration. The spindle rotation spanned the frequency range of robot modes in question. Mohammadi and Ahmadi [11] investigated two OMA methods where in-process FRFs are measured by leveraging milling forces as the excitation source. They proposed two approaches: (i) milling of porous materials to generate randomized cutting forces (achieing broadband, uncorrelated, and sufficiently exciting forces that can be considered as random), and (ii) milling of homogeneous material with spindle speed sweep (using the periodic content of cutting forces for excitation). In the work of Deng et al. [12], the FRF prediction approach is divided into two major steps. Firstly, the static FRFs are obtained from the EMA for different robot poses and are used to train a Gaussian process regression (GPR) model to predict the static FRF for different robot configurations. Robot joint angles are used as predictor variables and modal frequencies, damping ratios, and modal forms as response variables. Afterwards, these modal parameters for a static FRF predicted using GPR and the modal parameters identified by OMA were used to calculate the in-process FRFs of the robot in the operational state and refine the results.

Mohammadi and Ahmadi [13] propose another type of EMA that uses a shaker to apply a sinusoidal uni-directional excitation with a constant amplitude, performing a frequency sweep in the range of robot mode frequencies to examine the hypothesis of linearity of robot behavior. The obtained results suggest a clearly non-linear behavior, manifesting in evolution of modal frequencies, damping ratios, and corresponding FRF peaks as functions of the excitation force amplitude. The authors apply Nonlinear Complex Mode Analysis and derive empirical dependencies between the modal frequencies, damping ratios, FRF peak amplitudes, and excitation amplitudes using a non-linear function. It was shown that the FRFs obtained using this method differ from those obtained by the hammer impact method in terms of amplitudes. Other studies [7, 6, 14] report a violation of cross-FRF reciprocity, also suggesting non-linear robot behavior. The article [15] proposes a non-linear single degree of freedom model for the tool support. The form of the non-linear term was identified from experimental data and represented by cubic stiffness and damping terms. It was shown that the chosen model is capable of capturing the non-linear behavior of the robot, which includes the dependence of modal frequencies, damping ratios, and FRF amplitudes on the excitation amplitude.

he above assessment of the currently used methods for milling robots' modal analysis shows two main directions chosen by researchers: impact hammer testing and operational modal analysis using cutting forces for vibration excitation. Impact hammer testing is a relatively simple method that allows for broad-band excitation of robot dynamics and the obtaining of initial results in a relatively short time. However, this approach has a drawback when applied to dynamic systems whose behavior might be sufficiently non-linear to influence the outcome of the process in question, as reported in the case of a robotic arm used for milling. In fact, the widely used manual hammer impact testing is prone to variability in excitation levels, as a human hand cannot ensure a consistent level of energy injected into the system with each impact. This variability

aggravates the repeatability of the excitation, which, in the context of possible non-linear behavior, means that the nonlinearities of the studied system are excited at different levels. Moreover, the peak form of the excitation is far from the typical form of the cutting forces observed during the milling process. Additionally, as discussed above, hammer impact testing is most often performed with the robot halted, not taking into account the phenomena influencing robot dynamics during machining.

Operational modal analysis relying on milling forces aims to reproduce cutting conditions as closely as possible, resulting in more precise robot characterization. However, this approach requires cumbersome preparation before performing the modal analysis, such as identifying the cutting law coefficients (if a mechanistic description of the cutting forces is used) or using a dynamometric table for cutting force measurements (whose dynamic behavior can influence the modal analysis process). Additionally, the design of the OMA experiments involves choosing the machined workpiece and tool-material pair. This process must be repeated for each robot configuration in question.

The present article proposes a method that aims to find a niche between hammer impact tests and OMA methods. In the proposed method, the excitation comes from an unbalanced tool connected to the robot spindle, whose rotation speed sweeps through a range of frequencies that include the modal frequencies of the robot in question. This approach moves a step forward from impact hammer testing towards OMA, making it closer to an actual milling process while requiring less instrumentation than OMA. The rest of the article is organized as follows: Section 2 explains the proposed method and presents the experimental setup. Then, in Section 3, the methods used for recorded signal treatment are presented and the demodulation method used for FRF extraction is explained. Section4 presents the results of applying the proposed method to experiments with different values of unbalance, as well as a comparison with the FRF obtained using the manual impact hammer method. Finally, Section 5 discusses the results and further developments.

2 Methodology and experimental setup

The proposed method uses the rotation of the robot spindle with different values of unbalance to excite vibrations and further extract the dynamic parameters of the robot. Another advantage of this method is that, by choosing different values of unbalance, it is possible to apply excitation forces of a magnitude similar to the cutting forces applied to the robot during machining. This allows exciting the robot nonlinearities at a similar level as during actual machining.

The robot subjected to testing is the Staubli RX-170 HSM. This robot features a standard robotic arm with a spherical wrist layout, where the first five joints are cylindrical, and the sixth joint is replaced by a spindle for rotating the mill.

The full experimental setup is presented in Figure 1. It consists of the unbalanced tool ((a) in Figure 1b), created from a cylindrical blank tool (presumed to be initially perfectly balanced) with a radius of 20 mm, taken as the value of eccentricity, and a set of hose clamps (the mass of the non-axisymmetric part of each hose clamp is 4 g) mounted on the tool to create different values of unbalance. The unbalanced tool is then rotated at different spindle rotating speeds within a given range, exciting the vibrations of the robot. The accelerometers used are Kistler tri-axial 8763B500BB (1), (3), and uni-axial 8702B500M1 (2), fixed at different spots on the robot using wax to capture its vibrations during the test. The points of sensor placement and the directions of measurements are shown in Figure 1b. The tri-axial sensor (1) is placed on the stator part of the spindle such that its x-direction is parallel to axis 5 of the robot, its y-direction is parallel to the spindle rotation axis, and its z-direction is tangent to the surface of the stator at the point of sensor placement. The uni-axial sensor (2) is mounted on the 4th link of the robot, with its measurement direction perpendicular to the surface of the link. The tri-axial sensor (3) is placed on the 3rd link of the robot such that its x-direction is perpendicular to the link's surface, its y-direction is parallel to axis 3, and its z-direction is parallel to link 3.

Since the spindle mounted on the robot doesn't contain encoder allowing the recording of the current spindle angular position, it is necessary to implement the spindle rotation counter to measure the period of spindle rotation and estimate the spindle speed and angular phase. Such a counter is implemented using the Keyence LK-G32 CCD laser (b in the Figure 1b) with LK-G5001PV controller which performs the displacement

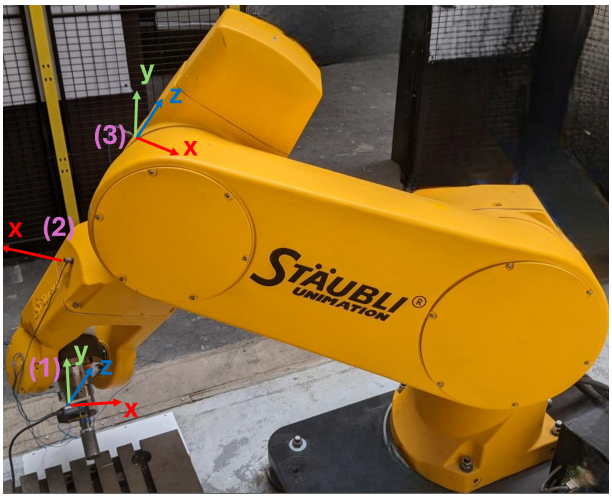

(a) Robot Staubli RX-170 HSM with the experimental set-up with sensor placement

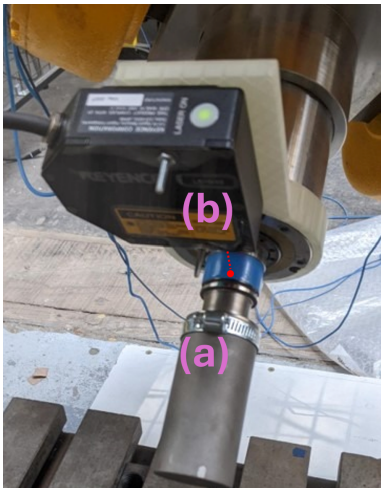

(b) Image of the unbalance (a), laser head (b) and laser spot

Figure 1: Experimental set-up

measurements and outputs the data in analogous form. The side of the tool, connected via the cone HSK-32 to the robot spindle, is located in the reference plane of the laser, the laser beam targets this reference plane. A special mark was left using a piece of an electrical tape, that covers one full circumference of the tool with a small overlap giving a small angular zone where the thickness of the tape is different. As a result, every time the mark goes under the laser spot the laser records a sudden continuous displacement change, a 'bump'. The mass of the mark is considered negligible with respect to the unbalance. The mark is left on the same angular position as the unbalances and they rotate synchronously. Thus, the bumps on the laser recordings mark every rotation and are uniquely related to the angular orientation of the unbalance and its phase (more details about this analysis can be found in the section 3). The laser head, the mark and the laser spot are presented in the Figure 1b. Laser sampling rate is taken to 20 kHz in order to be sure that there are enough instance laser spends on the mark for the highest tool spindle rate for better recording of the bump. All of the sensors are connected to the National Instrument cards NI 9234 via a chassis NI cDAQ-9174 that performs the signal digitizing and saves the data using Matlab Data Acquisition Toolbox.

Since the spindle mounted on the robot does not contain an encoder for recording the current spindle angular position, it is necessary to implement a spindle rotation counter to measure the period of spindle rotation and estimate the spindle speed and angular phase. The latter is important for extraction of the phase part of the response. This counter is implemented using the Keyence LK-G32 CCD laser (b in Figure 1b) with an LK-G5001PV controller, which performs displacement measurements and outputs the data in analog form. The side of the tool, connected via the cone HSK-32 to the robot spindle, is located in the reference plane of the laser, with the laser beam targeting this reference plane. A special mark was made using a piece of electrical tape that covers one full circumference of the tool with a small overlap, creating a small angular zone where the tape's thickness differs. As a result, every time the mark passes under the laser spot, the laser records a sudden continuous displacement change, or 'bump'. The mass of the mark is considered negligible with respect to the unbalance. The mark is placed in the same angular position as the unbalances, and they rotate synchronously. Thus, the bumps in the laser recordings mark each rotation and are uniquely related to the angular orientation of the unbalance and its phase (more details about this analysis can be found in Section 3). The laser head, the mark, and the laser spot are presented in Figure 1b. The laser sampling rate is set to 20 kHz to ensure sufficient instances of the laser passing over the mark for the highest tool spindle rate, allowing better recording of the bump. All sensors are connected to the National Instruments NI 9234 cards via a chassis NI cDAQ-9174, which performs synchronization, signal digitizing and stores the data using the Matlab Data Acquisition Toolbox.

The unbalance load is generated *via* a tool with known unbalance level is used to induce centrifugal force at the tool location. At constant rotating speed a steady monoharmonic load with a characteristic spatial distri-

bution is induced, composed of a pair of orthogonal components, phase-shifted by 90°. In our application these two components are applied to the tool (Figure 1). It should be highlighted that in case of unbalance excitation, to the difference of classical sine sweep tests, the input force magnitude is not constant, but proportional to the rotation frequency squared. In the present analysis we assume this location equivalent to that of the triaxial sensor 1 (shown in Figure 1a), in directions X and Z respectively:

$$F_X = U\omega^2 \cos(\omega t + \varphi), \quad F_Z = U\omega^2 \sin(\omega t + \varphi), \tag{1}$$

with F_X, F_Z corresponding force components (N), U unbalance (kg m), ω angular speed (rad/s) and φ unbalance angular location (deg). In the present set-up the 4 levels of unbalance are used $U \in \{u,\ 2u,\ 3u,\ 4u\}$, with the unit unbalance $u = 8 \cdot 10{-}5$ (kg m) induced by one hose clamp (Figure 1). These values allows obtaining the load of a magnitude similar to the cutting forces during the milling experiments performed on this robot.

The method to obtain the modal parameters of the robot involves a spindle rotation speed sweep across a range of frequencies of interest from the perspective of robot dynamics. The desired spindle speed evolution is set using the Val3 programming language for the robot and then interpreted by the spindle controller. The Val3 command accepts a value in bits, where 2^{15} bits span the entire possible spindle rotation speed range from 0 to 20,000 rpm. This setup imposes a spindle speed discretization from the controller side, with the minimal possible difference between two spindle speeds equal to 1 bit or approximately 0.01 Hz. The spindle rotation sweep is conducted by incrementing the desired spindle speed bit by bit in a loop and using the Val3 delay() command, which pauses the compilation and execution of the next line of the program, thus delaying the passage to the next iteration of the loop. By adjusting the value of the delay() command, it is possible to set different spindle rotation speed sweep rates. In the present study duration of one sweep was set to 4 minutes as a compromise between the time of the test and the influence of the sweep rate on the extracted FRF.

The value of the robot joint angles θ_i defining the pose of the robot are provided in Table 1. The angles are defined such that the vertical straight position of the robot corresponds to the all angles equal to zero. For all the results presented in this article, the robot is kept in this pose by its motors under the tension. It worth mentioning that the tests with the robot's brakes on showed no significant difference.

Table 1: Values of the robot joint angles, deg

θ_1	θ_2	θ_3	θ_4	θ_5
-23.76	70.85	74.32	54.95	77.41

3 Signal Analysis and FRF extraction techniques

Rather than using discrete Fourier transform for FRF extraction during the unbalance sweep test, demodulation [16, 17] was used to estimate the FRF of the recorded data. This method requires prior knowledge of the frequency ω of the input signal. In the present test, this frequency corresponds to the spindle rotation speed and is estimated using the implemented spindle rotation counter (bumps recorded by the laser as described in Section 2). The recorded accelerometer signal $x(t) = q_{1c}\cos(\omega t) - q_{1s}\sin(\omega t)$ is then multiplied by quadrature components:

$$\begin{aligned} (q_{1c}\cos(\omega t) - q_{1s}\sin(\omega t)) * \cos(\omega t) &= \tfrac{1}{2}\left(q_{1c} + q_{1c}\cos(2\omega t) - q_{1s}\sin(2\omega t)\right) \\ (q_{1c}\cos(\omega t) - q_{1s}\sin(\omega t)) * -\sin(\omega t) &= \tfrac{1}{2}\left(q_{1s} - q_{1s}\cos(2\omega t) - q_{1c}\sin(2\omega t)\right) \end{aligned} \tag{2}$$

This results in extraction of a sum of a static component proportional to the amplitude of the reference accelerometer signal in $y(t)$ and an oscillating part corresponding to the frequency $2\omega t$. The oscillating part can be removed using a low-pass filter, as described in Figure 2, which controls the selectivity around the target frequency. This step linearizes the robot's frequency response function on the unbalanced excitation around

the value of this excitation. To obtain the classical robot FRF, it is necessary to divide this characteristic by $U\omega^2$. Every figure featuring an FRF obtained by the demodulation uses this latter formulation.

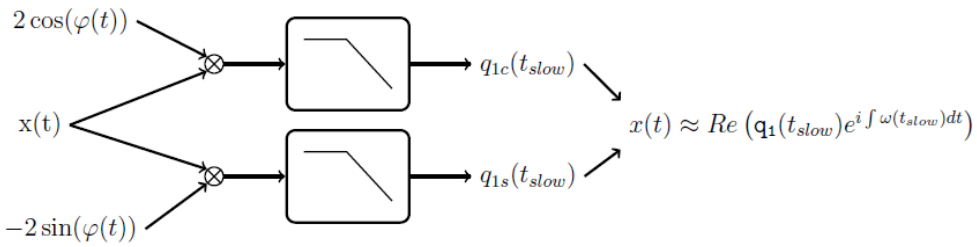

Figure 2: Diagram showing the synchronous demodulation algorithm

Figure 3a shows a portion of the extracted tool rotation frequency using the spindle rotation counter data recorded during a sweep unbalance test. This is done by taking the inverse of the time periods between neighboring bumps. It is visible that the spindle speed is actually updated at a low frequency around 10 Hz with imperfect control. However, this does not significantly affect the spectrogram or the ability to estimate the first three harmonics reliably as shown in Figure 4. Applying this extracted instantaneous frequency for the demodulation (equation (2) and Figure 2) results in a noisy FRF. Figure 3b features the zoomed-in portion of the FRF for the test with $U = 4u$ for three directions of the triaxial accelerometer (1) 1:x, 1:y and 1:z. The effect of spindle speed control discussed above can be seen; however, these FRFs can give an idea about the modal frequencies. Thus, it was decided to further use the approximated instantaneous frequency (dashed line in Figure 3a found by linear regression of the extracted instantaneous spindle frequency.

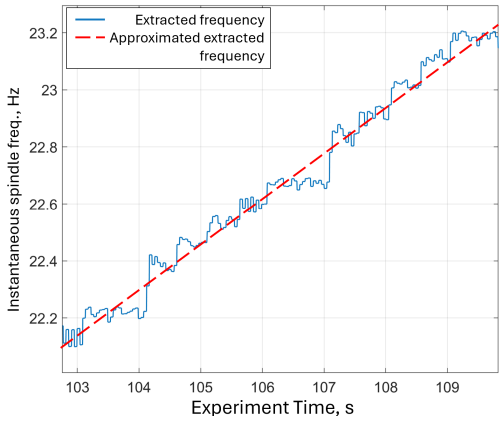

(a) Spindle instantaneous rotational frequency

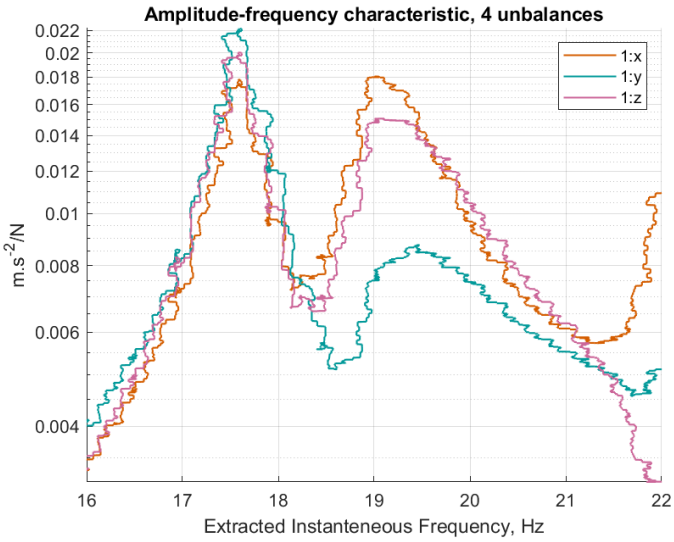

(b) Resulting FRFs for three sensor data 1:x, 1:y, 1:z using the non-approximated extracted spindle rotation frequency

Figure 3: Influence of the extracted instantaneous spindle speed on the results of the demodulation

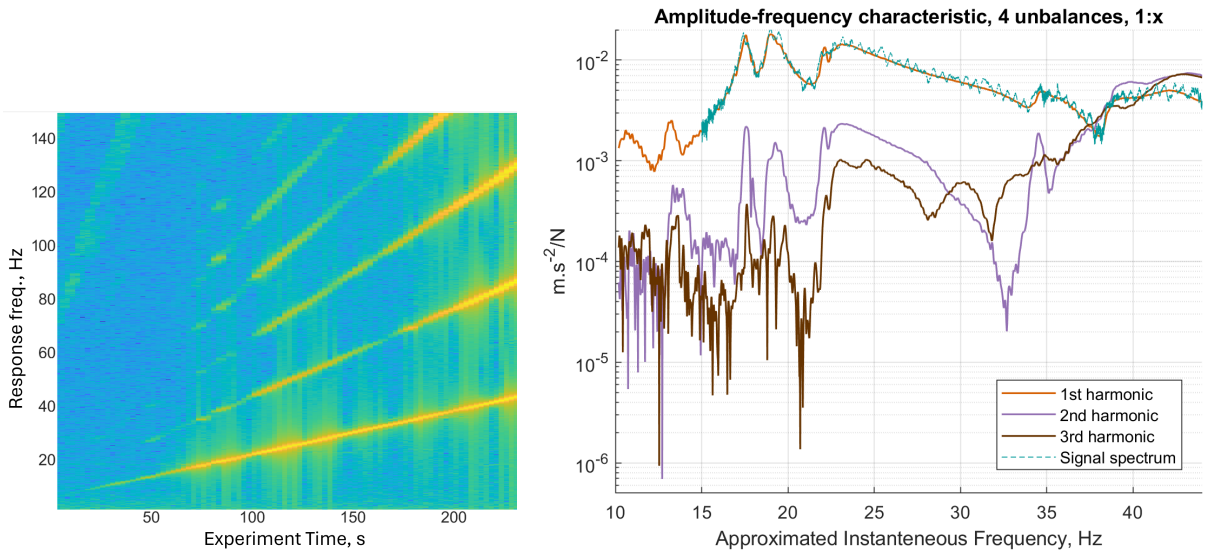

(a) Spectrogram of the recorded 1:x data for test with 4 unbalances

(b) First three harmonics of the FRF for 1:x data for $U = 4u$ and the normalized spectrum of the signal

Figure 4: Estimation of the harmonics for 1:x data for the test with 4 unbalances

Figure 4a shows the spectrogram of the signal recorded by the x-direction of the triaxial accelerometer (1) denoted 1:x under sweep unbalanced excitation with $U = 4u$. The main harmonic as well as the higher harmonics of the robot FRF are visible. Figure 4b shows the first three harmonics found by the demodulation in the frequency range [10, 45] Hz. It can be seen that in the frequency range of interest, the higher harmonics are generally of a smaller order compared to the main harmonic. Thus, they can be neglected allowing the comparison of the first harmonic with the form of the signal spectrum (also presented as well in Figure 4b). The latter is obtained taking the FFT of the signal and normalizing its frequency content by the factor of $U\omega^2$. As can be seen, the spectrum, though having some similarities, is much noisier (its content below 15 Hz is hidden to avoid obscuring the figure) and loses some of the peaks.

4 Results

The introduced technique was applied to investigate the robot non-linear behavior using four different levels of unbalance $U \in \{u, 2u, 3u, 4u\}$. It has been reported that the main robot modes are typically located in the range below 40 Hz [7]; thus, this range is studied in the present work.

Figure 5a presents the the evolution of FRF for the data 1:x for different level of unbalance obtained using demodulation. The plots suggest a clear non-linear behavior of the system that depends on the amplitude of the excitation. The pole tracking capabilities of SDT software [18, 19] were used to identify the modes of the robot for each of the value of the unbalance U, considering each case as a linearized system. Figure 5b shows the evolution of the identified poles of these linearized systems (modal frequency - damping ratio) with the value of the unbalance U. All modes exhibit softening behavior, and the damping usually increases with amplitude.

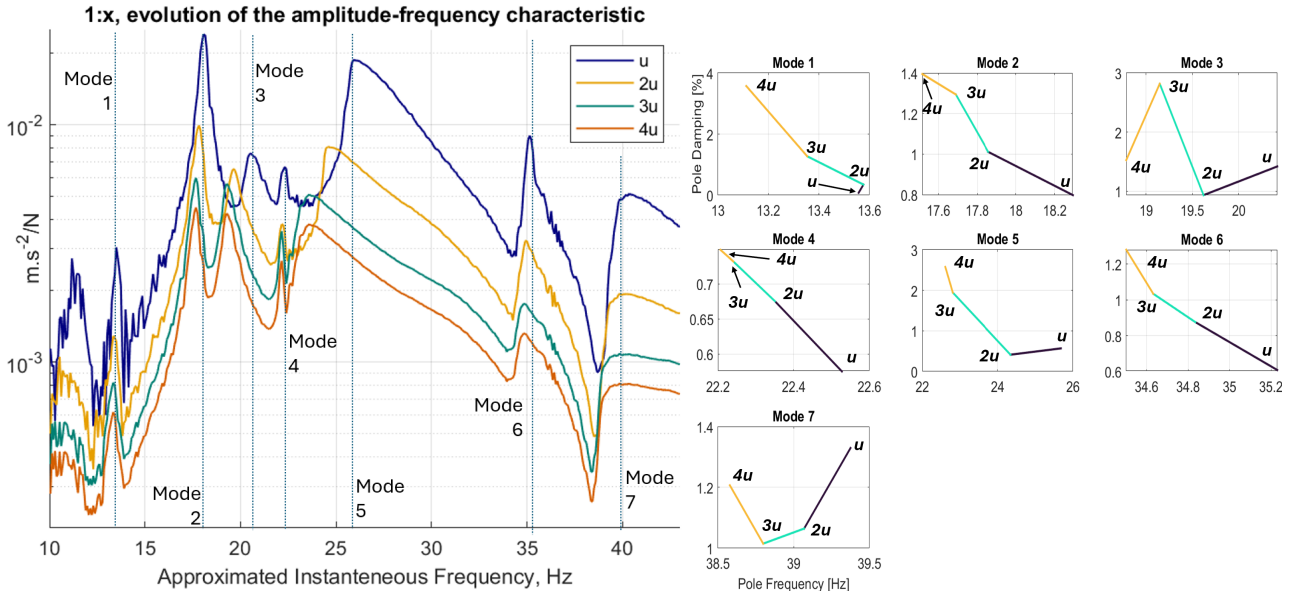

(a) Evolution of the extracted FRF for the data 1:x depending on the value of the unbalance U

(b) Evolution of the identified poles depending on the value of the unbalance U

Figure 5: Influence of the unbalance U on the response of the sensor 1:x

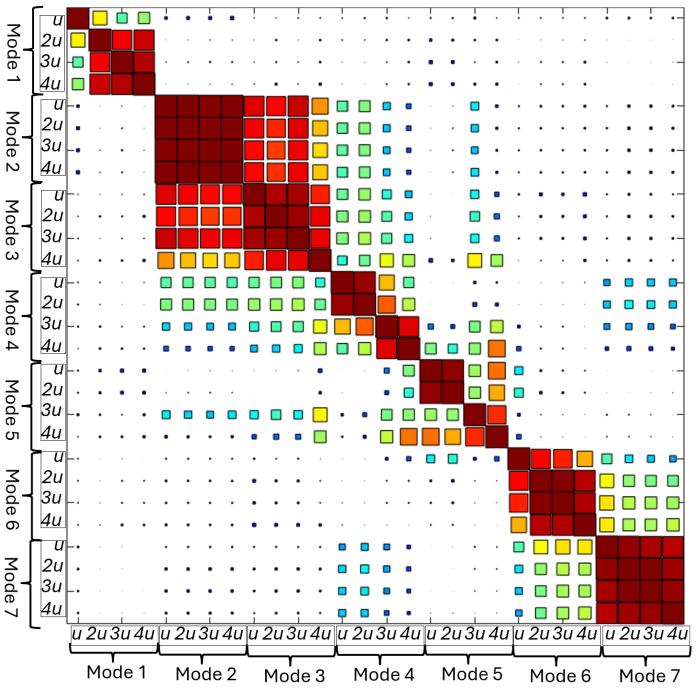

Figure 6: Block MAC for four values of the unbalance U

Speaking about the modal shapes, that were obtained using the data of all sensors (1), (2), (3), the block auto-MAC shown in Figure 6 illustrates fairly good shape stability. Each block contains the correlation of the same mode for four values of the unbalance U, and thus it is expected to have seven blocks composed of 4 sub-blocks of well correlated shapes. Analysing the results, generally, each block contains well-correlated sub-blocks, indicating that for the used values of the unbalance U, the poles are indeed shifted and no mode swapping occurs. However, for some modes, the results are worse. This can be explained in two ways. First, as seen in Figure 5a, some peaks become closer with the rise of U (e.g. peaks 2 and 3, and 4 and 5) suggesting that the corresponding mode shapes may undergo some changes as well. On the other hand, modes 3-4 have

very similar shapes when observed from the all seven used sensors, even for the same value of the unbalance $U = u$ so that more sensors are necessary to distinguish these modes. Analysis of the correlation losses (e.g. first mode for $U = u$; forth mode for $U = u$ or $2u$ versus $U = 3u$ or $4u$) should be further performed with errors defined by mode/sensor [20].

5 Conclusions

A new modal analysis method for investigating the dynamic behavior of milling robots is presented. The method leverages the inertial forces generated by an unbalanced tool rotating on the spindle to excite vibrations. Based on the accelerometer data, the frequency response function (FRF) was obtained using the demodulation technique.

It was shown that this method outperforms the approach of using the FFT of the sensor data in terms of a better signal-to-noise ratio and reveals more spectral details. Using this method, the evolution of the robot's FRF with respect to the value of the unbalance was demonstrated. The modes of the system, linearized around each value of the unbalance, exhibit softening behavior and an increase in damping as the value of the unbalance increases. It was also shown that for the used values of the unbalance, no mode swapping occurs. However, further investigations with higher levels of unbalance are required to further examine this aspect. Additionally, more sensors are necessary for more precise identification of the modes. This variation in robot behavior suggests the presence of some form of nonlinearity that needs to be further investigated. Thus, this work demonstrates the potential of the proposed method, which can find its niche among other widespread modal analysis techniques because it allows for excitation level control in contrast with impact hammer testing and requires less instrumentation than OMA methods. However, it needs further development. Notably, the quality of the extracted FRF depends on the quality of the extracted spindle rotation speed, as it is used as a key parameter for demodulation. As shown in this work, a relatively simple rotation analysis with one count per turn allows to obtain FRFs and to extract modal features un a given load magnitude range. To ensure the better results, both the spindle control loop and the method used to record the spindle speed data should be taken into account.

The proposed method can be used for semi-automatic characterization of the robot in a set of different poses. Finally, as the unbalance performs only planar motion, the question of excitation in the third direction remains. The presented method and obtained results, enable assessing the nonlinear behavior of the robot with respect to the magnitude of the external loading. These features can potentially impact the robotic milling operation, and the accounting for these them in machining simulations is yet to be carried out.

References

[1] C. Dumas, S. Caro, M. Chérif, S. Garnier, and B. Furet, "A methodology for joint stiffness identification of serial robots," in *2010 IEEE/RSJ International Conference on Intelligent Robots and Systems*. Taipei: IEEE, Oct. 2010, pp. 464–469. [Online]. Available: http://ieeexplore.ieee.org/document/5652140/

[2] C. Dumas, S. Caro, S. Garnier, and B. Furet, "Joint stiffness identification of six-revolute industrial serial robots," *Robotics and Computer-Integrated Manufacturing*, vol. 27, no. 4, pp. 881–888, Aug. 2011. [Online]. Available: https://linkinghub.elsevier.com/retrieve/pii/S0736584511000342

[3] A. Olabi, "Amélioration de la précision des robots industriels pour des applications d'usinage a grande vitesse," Theses, Arts et Métiers ParisTech, Nov. 2011, issue: 2011ENAM0034. [Online]. Available: https://pastel.archives-ouvertes.fr/pastel-00649019

[4] J. Li, B. Li, N. Shen, H. Qian, and Z. Guo, "Effect of the cutter path and the workpiece clamping position on the stability of the robotic milling system," *The International Journal of Advanced Manufacturing Technology*, vol. 89, no. 9-12, pp. 2919–2933, Apr. 2016. [Online]. Available: http://link.springer.com/10.1007/s00170-016-9759-x

[5] S. Mousavi, V. Gagnol, B. C. Bouzgarrou, and P. Ray, "Dynamic modeling and stability prediction in robotic machining," *The International Journal of Advanced Manufacturing Technology*, vol. 88, no. 9-12, pp. 3053–3065, Feb. 2017. [Online]. Available: http://link.springer.com/10.1007/s00170-016-8938-0

[6] M. Cordes, W. Hintze, and Y. Altintas, "Chatter stability in robotic milling," *Robotics and Computer-Integrated Manufacturing*, vol. 55, pp. 11–18, Feb. 2019. [Online]. Available: https://linkinghub.elsevier.com/retrieve/pii/S073658451830084X

[7] H. H. Nam, "Robotic machining: Development and validation of a numerical model of robotic milling to optimise the cutting parameters," Ph.D. dissertation, UNIVERSITY OF MONS, 2019, publisher: Unpublished. [Online]. Available: http://rgdoi.net/10.13140/RG.2.2.32268.46726

[8] H. Cai, B. Luo, X. Mao, L. Gui, B. Song, B. Li, and F. Peng, "A Method for Identification of Machine-tool Dynamics under Machining," *Procedia CIRP*, vol. 31, pp. 502–507, 2015. [Online]. Available: https://linkinghub.elsevier.com/retrieve/pii/S2212827115002255

[9] B. Altun, H. Çalışkan, and O. Özşahin, "Position-dependent FRF identification without force measurement in milling process," *The International Journal of Advanced Manufacturing Technology*, vol. 128, no. 11-12, pp. 4981–4996, Oct. 2023. [Online]. Available: https://link.springer.com/10.1007/s00170-023-11925-w

[10] A. Iglesias, J. Munoa, C. Ramírez, J. Ciurana, and Z. Dombovari, "FRF Estimation through Sweep Milling Force Excitation (SMFE)," *Procedia CIRP*, vol. 46, pp. 504–507, 2016. [Online]. Available: https://linkinghub.elsevier.com/retrieve/pii/S221282711630155X

[11] Y. Mohammadi and K. Ahmadi, "In-Process Frequency Response Function Measurement for Robotic Milling," *Experimental Techniques*, vol. 47, no. 4, pp. 797–816, Aug. 2023. [Online]. Available: https://link.springer.com/10.1007/s40799-022-00590-5

[12] K. Deng, D. Gao, C. Zhao, and Y. Lu, "Prediction of in-process frequency response function and chatter stability considering pose and feedrate in robotic milling," *Robotics and Computer-Integrated Manufacturing*, vol. 82, p. 102548, Aug. 2023. [Online]. Available: https://linkinghub.elsevier.com/retrieve/pii/S0736584523000248

[13] Y. Mohammadi and K. Ahmadi, "Structural Nonlinearity of Robotic Machining Systems," in *Volume 2: Manufacturing Processes; Manufacturing Systems; Nano/Micro/Meso Manufacturing; Quality and Reliability*. Virtual, Online: American Society of Mechanical Engineers, Sep. 2020, p. V002T09A009. [Online]. Available: https://asmedigitalcollection.asme.org/MSEC/proceedings/MSEC2020/84263/Virtual,%20Online/1095800

[14] Y. Mohammadi and K. Ahmadi, "Effect of axial vibrations on regenerative chatter in robotic milling," *Procedia CIRP*, vol. 82, pp. 503–508, 2019. [Online]. Available: https://linkinghub.elsevier.com/retrieve/pii/S2212827119308820

[15] Y. Mohammadi and K. Ahmadi, "Single Degree-of-Freedom Modeling of the Nonlinear Vibration Response of a Machining Robot," *Journal of Manufacturing Science and Engineering*, vol. 143, no. 051003, Nov. 2020. [Online]. Available: https://doi.org/10.1115/1.4048513

[16] M. Feldman, "Hilbert transform in vibration analysis," *Mechanical Systems and Signal Processing*, vol. 25, no. 3, pp. 735–802, Apr. 2011.

[17] G. Malacrida Alves, E. Balmes, G. Martin, G. Vermot Des Roches, D. Zhang, and T. Chancelier, "An harmonic balance vector signal model to study slow parametric sensitivity of brake squeal occurrences," *MSSP*, vol. Submitted to, 2023.

[18] N. Benbara, G. Martin, M. Rébillat, and N. Mechbal, "Bending waves focusing in arbitrary shaped plate-like structures: Study of temperature effects, development of a digital twin and of an associated neural-network based compensation procedure," *Journal of Sound and Vibration*, vol. 526, p. 116747, May 2022.

[19] *Structural Dynamics Toolbox (for Use with MATLAB)*. Paris: SDTools, 1995-2024.

[20] G. Martin, E. Balmes, and T. Chancelier, "Characterization of identification errors and uses in localization of poor modal correlation," *Mechanical Systems and Signal Processing*, vol. 88, pp. 62–80, May 2017.